Crystal Structure of $Cs_2V_4O_{11}$ with Unusual V–O Coordinations

Yoshio Oka,* Fumihiko Saito,† Takeshi Yao,† and Naoichi Yamamoto‡

*Department of Natural Environment Sciences, Faculty of Integrated Human Studies, †Department of Fundamental Energy Science,
Graduate School of Energy Sciences, and ‡Graduate School of Human and Environmental Studies, Kyoto University, Kyoto 606, Japan*

Single crystals of $Cs_2V_4O_{11}$ were obtained in the hydrothermal $CsVO_3$–$VO(OH)_2$ system and its structural chracterization was performed. $Cs_2V_4O_{11}$ crystallizes in the *C*-centered orthorhombic system: *Cmm*2 with $a = 5.571(2)$ Å, $b = 9.639(2)$ Å, $c = 5.222(2)$ Å and $Z = 1$. Structure refinements based on 402 reflections converged to $R = 0.037$ and $R_w = 0.044$. The structure has V_4O_{11} layers and interlayer Cs atoms. The V_4O_{11} layer exhibits an unusual V–O network structure consisting of VO_4 tetrahedra and VO_5 trigonal bipyramids in a random distribution. The structure is derived from that of a fictive V_4O_{10} layer made up of vertex-sharing VO_4 tetrahedra. That is, one-fourth of the shared vertices in the V_4O_{10} layer are converted into shared edges by adding extra oxygens leading to the V_4O_{11} layer; actually a vertex-sharing VO_4 dimer changes to an edge-sharing VO_5 dimer. Consequently the V atom in a single crystallographic site shows two different V–O coordinations of VO_4 tetrahedra and VO_5 trigonal bipyramids in a one-to-one ratio. © 1997 Academic Press

INTRODUCTION

In the V_2O_5–Cs_2O phase diagram for $0 \leq Cs/V \leq 1$, three cesium vanadate phases have been reported to exist, namely $CsVO_3$, CsV_3O_8, and $Cs_2V_4O_{11}$ (1–3). Among these phases $CsVO_3$ and CsV_3O_8 are well characterized structurally, and their isomorphous phases have also been produced by replacing Cs with K, Rb, NH_4, and Tl (4–8). $CsVO_3$ crystallizes in the orthorhombic system *Pbcm*: $a = 5.393$ Å, $b = 12.249$ Å, and $c = 5.786$ Å, and consists of vertex-sharing VO_4 tetrahedral chains running along the *c* axis (4). CsV_3O_8 adopts a layered structure with monoclinic symmetry $P2_1/m$: $a = 5.0029$ Å, $b = 8.543$ Å, $c = 8.2021$ Å, and $\beta = 95.56°$, in which V_3O_8 layers made up of VO_6 octahedra and VO_5 trigonal bipyramids stack along the *c* axis (5, 8). On the other hand, only little is known about $Cs_2V_4O_{11}$. The compound was first reported in the V_2O_5–Cs_2O phase diagram by Belyaev and Golovanova (1), to exist in a limited temperature range of 380 to 446°C below which a two-phase state $CsVO_3$–CsV_3O_8 was claimed to appear. The phase diagram reinvestigated by Perraud (2), however, demonstrated the stability of $Cs_2V_4O_{11}$ below 380°C, denying

the two-phase field or region. Later on, the revised diagram was confirmed by Forslund (3). Perraud also reported the *C*-centered orthorombic system with $a = 9.764$ Å, $b = 5.596$ Å, and $c = 10.530$ Å (corrected to match the X-ray diffraction data given in Ref. (2)) and a reversible transition at 380°C to an unidentified high-temperature phase (2). It is of interest to determine the structure of $Cs_2V_4O_{11}$; however, according to the phase diagram (2, 3) single-crystal growth from the melt seems to be difficult. In the present study we have succeeded in synthesizing single crystals of $Cs_2V_4O_{11}$ by hydrothermal methods and report its structural characterization. The structure reveals a layer type consisting of V_4O_{11} where the V atom has unusual V–O coordinations.

EXPERIMENTAL

Sample Preparation

The hydrothermal system of $VO(OH)_2$–$CsVO_3$ was employed, where $VO(OH)_2$ powders were obtained by hydrothermal treatment of $VOSO_4$–NaOH suspensions at 150°C and $CsVO_3$ powders by heat treatment at 500°C of dried-up powders of Cs_2CO_3 and NH_4VO_3 solutions with $Cs/V = 1.0$. $CsVO_3$ and $VO(OH)_2$ powders (total 5.0 g with $V/Cs \approx 1.2$) dispersed in 50 ml distilled water were placed in a sealed Pyrex ampoule and treated in an autoclave at 280°C for 30 h. Precipitates were filtered out and yellow prismatic crystals were subsequently separated from black fine powders by repeated ultrasonic agitation and decantation. Yellow crystals were identified as the low-temperature $Cs_2V_4O_{11}$ reported by Perraud (2) using powder X-ray diffractometry and their Cs/V atomic ratio was confirmed to be 0.5 by energy-dispersive X-ray (EDX) analysis. Black powders showed the Cs/V ratio of about 1/3 with a significant amount of Si presumably extracted from Pyrex glass but their exact compositions as well as crystalline phases remain unknown. The hydrothermal system of V_2O_5–$CsVO_3$ produced CsV_3O_8 crystals instead of $Cs_2V_4O_{11}$. As a reference material $Cs_2V_4O_{11}$ powders were prepared by solid-state reaction of Cs_2CO_3 and V_2O_5 powders, which were heated at 430°C for 158 h followed by furnace cooling. The product was confirmed to be Perraud's

low-temperature $Cs_2V_4O_{11}$ phase (2) with a trace of CsV_3O_8 by powder X-ray diffractometry.

Single-Crystal X-ray Diffraction

A single crystal of $Cs_2V_4O_{11}$ with dimensions $0.2 \times 0.1 \times 0.1$ mm was mounted on a Rigaka AFC-7R diffractometer with monochromatized $MoK\alpha$ radiation. $Cs_2V_4O_{11}$ crystallizes in the C-centered orthorhombic system with cell parameters of $a = 5.571(2)$ Å, $b = 9.639(2)$ Å, and $c = 5.222(2)$ Å determined from 22 reflections of $25.0° < 2\theta < 29.8°$. Data collection was carried out up to $2\theta = 80°$ by the 2θ-ω scanning technique with a scan width $\Delta\omega = (1.47 + 0.30 \tan\theta)°$, and three standard reflections monitored every 150 data showed no significant intensity fluctuations. A total of 534 reflections were collected, of which 402 reflections with $I > 3\sigma(I)$ were used in the structure refinements. An empirical absorption correction of the ψ-scan method was applied to yield transmission factors 0.889–1.000. All the data processing and structure refinement calculations were performed using the TEXSAN software package (9). Experimental and crystallographic data are listed in Table 1.

Structure Determination

The number of formula units is determined from the cell volume undoubtedly to be $Z = 1$ which apparently comes into conflict with the odd number of oxygens for the ordinary C-centered lattices. This problem has been solved as described below. Possible space groups are $Cmmm$, $C222$, $Cmm2$, and $Cm2m$. Cs and V atoms were easily located by direct methods for any choice of the space groups. The Cs sites for each possibility are common at $(0, 0, 0)$, and V sites can also be common at $(0, 0.672, 0.5)$ if the z parameter for $Cmm2$, actually $z = 0.492$, is fixed to 0.5. Oxygens were subsequently located for each space group in difference

TABLE 1
Crystallographic Data and Experimental Parameters for $Cs_2V_4O_{11}$

Space group	$Cmm2$
a (Å)	5.671(2)
b (Å)	9.639(2)
c (Å)	5.222 (2)
V (Å³)	285.5(1)
Z	1
D_c (g cm⁻³)	3.755
μ (cm⁻¹)	95.0
No. of unique reflections ($I > 0$)	534
No. of reflections ($I > 3\sigma(I)$)	402
No. of variables	25
R	0.036
R_w	0.043

TABLE 2
Atomic Parameters, Isotropic Temperature Factors, and Occupancies for $Cs_2V_4O_{11}$

Atom	Position	x	y	z	B_{eq}(Å²)	Occupancy
Cs	$2a$	0	0	0	2.31(1)	1
V	$4e$	0	0.6718(1)	0.4915(7)	2.47(2)	1
O(1)	$2b$	0	0.5	0.362(2)	2.4(2)	1
O(2)	$4e$	0	0.6654(6)	0.796(1)	2.6(1)	1
O(3)	$4c$	0.25	0.25	0.356(2)	1.7(1)	0.75
O(4)	$8f$	0.150(2)	0.142(1)	0.489(5)	1.5(2)	0.25

Fourier maps. As a result, $Cmm2$ gave the most plausible structure with O(1), O(2), and O(3), which, however, yielded the composition $Cs_2V_4O_{10}$. This structure has V_4O_{10} layers consisting of edge-sharing VO_4 tetrahedra as depicted in Fig. 1. The refinements converged to $R = 0.061$ and $R_w = 0.073$; however, this structure is not acceptable because of the inappropriate composition. Further search for oxygen atoms in difference Fourier maps detected two partially filled sites on both sides of the O(3) site at a distance of 1.4 Å. This suggested that O(3) in the $4c$ position partly splits into O(4) in the $8f$ position in a manner shown in Fig. 2. Sites occupancies of O(3) and O(4) were checked to give 0.76(3) and 0.23(2), respectively, and thus were fixed to 0.75 and 0.25, respectively, to fit the $Cs_2V_4O_{11}$ composition; Cs and V sites were confirmed to have full occupancies. The revised structure was refined to $R = 0.036$ and $R_w = 0.043$. The atomic parameters and isotropic temperature factors are given in Table 2. The anisotropic displacement factors are given in Table 3.

RESULTS AND DISCUSSION

Description of Structure

The disclosed structure of $Cs_2V_4O_{11}$ is depicted in Fig. 3. The structure consists of V_4O_{11} layers and interstitial Cs atoms. The striking structural feature is that the V atom in a single crystallographic site has two different V–O coordinations, namely VO_4 tetrahedron and VO_5 trigonal bipyramid. V–O bond distances and O–V–O angles for both

TABLE 3
Anisotropic Displacement Factors for $Cs_2V_4O_{11}$

Atom	U_{11}	U_{22}	U_{33}	U_{12}	U_{13}	U_{23}
Cs	0.0348(3)	0.0316(3)	0.0211(2)	0	0	0
V	0.0386(6)	0.0163(4)	0.0391(8)	0	0	0.009(1)
O(1)	0.047(5)	0.013(3)	0.033(4)	0	0	0
O(2)	0.044(3)	0.027(3)	0.026(3)	0	0	−0.002(2)
O(3)	0.011(2)	0.024(3)	0.030(3)	0.004(2)	0	0
O(4)	0.009(4)	0.016(4)	0.031(7)	0.004(3)	−0.007(9)	−0.008(10)
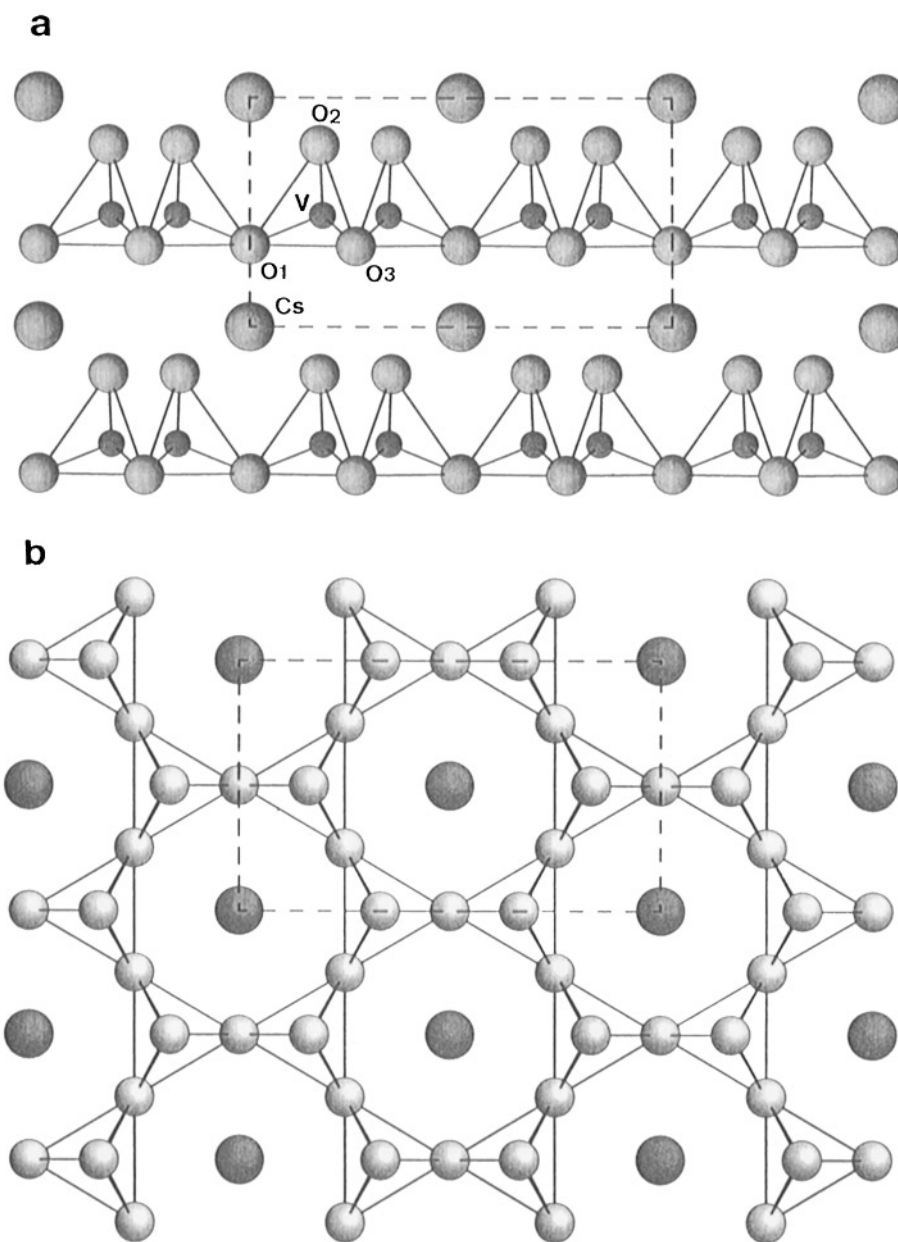
FIG. 1. Crystal structure of the fictitious or fictive compound "$Cs_2V_4O_{10}$" as a prototype of $Cs_2V_4O_{11}$ projected onto (a) the bc plane and (b) the ab plane. Unit cell is denoted by broken lines.

polyhedra are listed in Table 4. This situation arises from the splitting of one O(3) into two O(4) as demonstrated in Fig. 2, resulting in the conversion of two VO_4 tetrahedra sharing the O(3) vertex into two VO_5 trigonal bipyramids sharing the O(4)–O(4) edge. V–O coordinations around two adjacent V atoms are depicted in Fig. 4 where the vertex-sharing VO_4 dimer is formed with the shared O(3) vertex and the edge-sharing VO_5 dimer with the shared O(4)–O(4) edge. A quarter of O(3) exhibit the splitting, and consequently half of VO_4 tetrahedra are transformed to VO_5

trigonal bipyramids. Since no superstructure was observed, the edge-sharing VO_5 units distribute randomly in the V_4O_{11} layer. This unusual V–O coordination must cause the fracturing of the V position leading to the anomalously large B_{eq} value of 2.47(2) $Å^2$ for V, which is also the case for the O(1) and O(2) positions showing relatively large B_{eq} values of 2.4(2) and 2.6(1) $Å^2$, respectively. The interstitial Cs atom is nominally surrounded by 16 oxygens as depicted in Fig. 5 with Cs–O distances listed in Table 5; 20 oxygens are shown in Fig. 5 which are reduced to 16 because adjacent
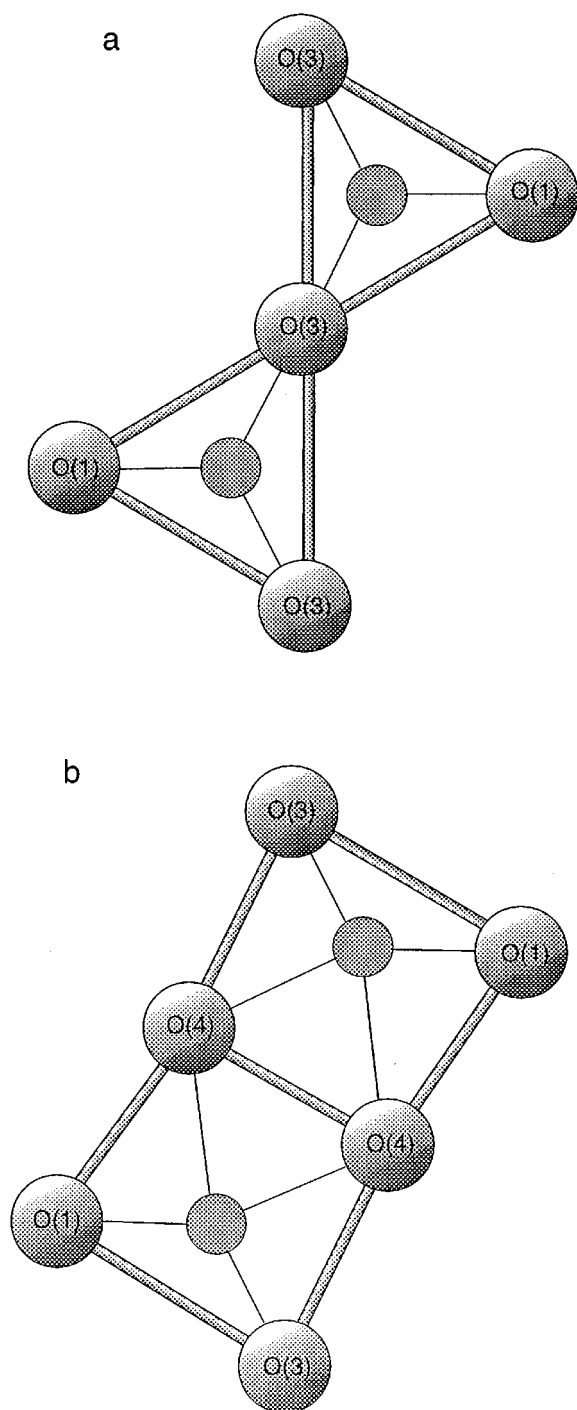
FIG. 2. Splitting of one O(3) in a $4c$ site into two O(4) in $8f$ sites: (a) before splitting; (b) after splitting.

TABLE 4
Bond Distances (Å) and Angles (°) for V–O Polyhedra in $Cs_2V_4O_{11}$

		VO_4 tetrahedron			
V–O(1)	1.788(5)	V–O(2)	1.59(1)	V–O(3)^{a,b}	1.755(5)
O(1)–V–O(2)		110.0(5)	O(1)–V–O(3)^{a,b}		104.2(3)
O(2)–V–O(3)^{a,b}		114.8(4)	O(3)–V–O(b)^{b}		107.8(4)
		VO_5 trigonal bipyramid			
V–O(1)	1.788(5)	V–O(2)	1.59(1)	V–O(3)$^{a \, or \, b}$	1.755(5)
V–O(4)^{e}	1.99(1)	V–O(4)^{d}	2.01(1)		
O(1)–V–O(2)		110.0(5)	O(1)–V–O(3)$^{a \, or \, b}$		104.2(3)
O(1)–V–O(4)^{c}		82.2(5)	O(1)–V–O(4)^{d}		145.5(9)
O(2)–V–O(3)$^{a \, or \, b}$		114.8(4)	O(2)–V–O(4)^{c}		92.4(8)
O(2)–V–O(4)^{d}		90.0(6)	O(3)$^{a \, or \, b}$–V–O(4)^{c}		87.4(5)
O(3)$^{a \, or \, b}$–V–O(4)^{d}		149.2(6)	O(4)^{c}–V–O(4)^{d}		72.9(6)

Note. Symmetry codes: ^{a} x, $y + \frac{1}{2}$, z; ^{b} $-x$, $y + \frac{1}{2}$, z; ^{c} x, $1 - y$, z or $-x$, $1 - y$, z; ^{d} $x - \frac{1}{2}$, $y + \frac{1}{2}$, z or $\frac{1}{2} - x$, $y + \frac{1}{2}$, z.

Comparison with $Cs_2V_4O_{11}$ of the $Cs_2O–V_2O_5$ Phase Diagram

Perraud revised the $Cs_2O–V_2O_5$ phase diagram and confirmed the stability region of $Cs_2V_4O_{11}$ (2). He also reported the orthorhombic system with $a = 9.764$ Å, $b = 5.596$ Å, and $c = 10.530$ Å (corrected to match the X-ray diffraction data given in Ref. (2)) denoting that the c axis of our cell dimensions is doubled. This suggests that some $2 \times c$ structure may be adopted by the sample prepared by solid state reaction. To check this point we have synthesized powder samples by solid state reaction of Cs_2CO_3 and V_2O_5 as described above. Figure 6 shows the powder X-ray pattern of the reference sample which is consistent with that reported by Perraud (2) but is completely indexed with our cell dimensions. Therefore the reference sample is identical to the Perraud's sample, or in other words the Perraud's pattern can be indexed with our cell dimensions. Moreover, as also shown in Fig. 6, the pattern of the reference sample agrees well with the pattern calculated from the crystallographic data. The results indicate the rejection of the Perraud's $2 \times c$ structure and the structural similarity between $Cs_2V_4O_{11}$ of the $Cs_2O–V_2O_5$ phase diagram and $Cs_2V_4O_{11}$ by the hydrothermal method.

TABLE 5
Cs–O Distances (Å) for Cs–O Polyhedron

Cs–O(b)^{a,b}	3.409(7)	Cs–O(2)^{c,d}	3.396(7)
Cs–O(2)^{e,f,g,h}	3.423(4)	Cs–O(3)^{i,j,k,l}	3.357(5)
Cs–O(4)^{m,o}	3.02(3)	Cs–O(4)^{p,q}	3.12(3)

Note. Symmetry codes: ^{a} $x - \frac{1}{2}$, $y - \frac{1}{2}$, z; ^{b} $x + \frac{1}{2}$, $y - \frac{1}{2}$, z; ^{c} x, $y - 1$, $z - 1$; ^{d} x, $1 - y$, $z - 1$; ^{e} $x + \frac{1}{2}$, $y - \frac{1}{2}$, $z - 1$; ^{f} $x - \frac{1}{2}$, $y - \frac{1}{2}$, $z - 1$; ^{g} $x - \frac{1}{2}$, $\frac{1}{2} - y$, $z - 1$; ^{h} $x + \frac{1}{2}$, $\frac{1}{2} - y$, $z - 1$; ^{i} x, y, z; ^{j} $-x$, $-y$, z; ^{k} $-x - y$, z; ^{l} x, $-y$, z; ^{m} x, y, z or $-x$, y, z; ^{o} $-x$, $-y$, z or x, $-y$, z; ^{p} x, y, $z - 1$ or $-x$, y, $z - 1$; ^{q} $-x$, $-y$, $z - 1$ or x, y, $z - 1$.

O(4) sites must not be occupied simultaneously. The actual coordination number differs from 11 to 14 due to partial occupancies of O(3) and O(4) sites, and the Cs–O polyhedron should be CsO_{13} on average.
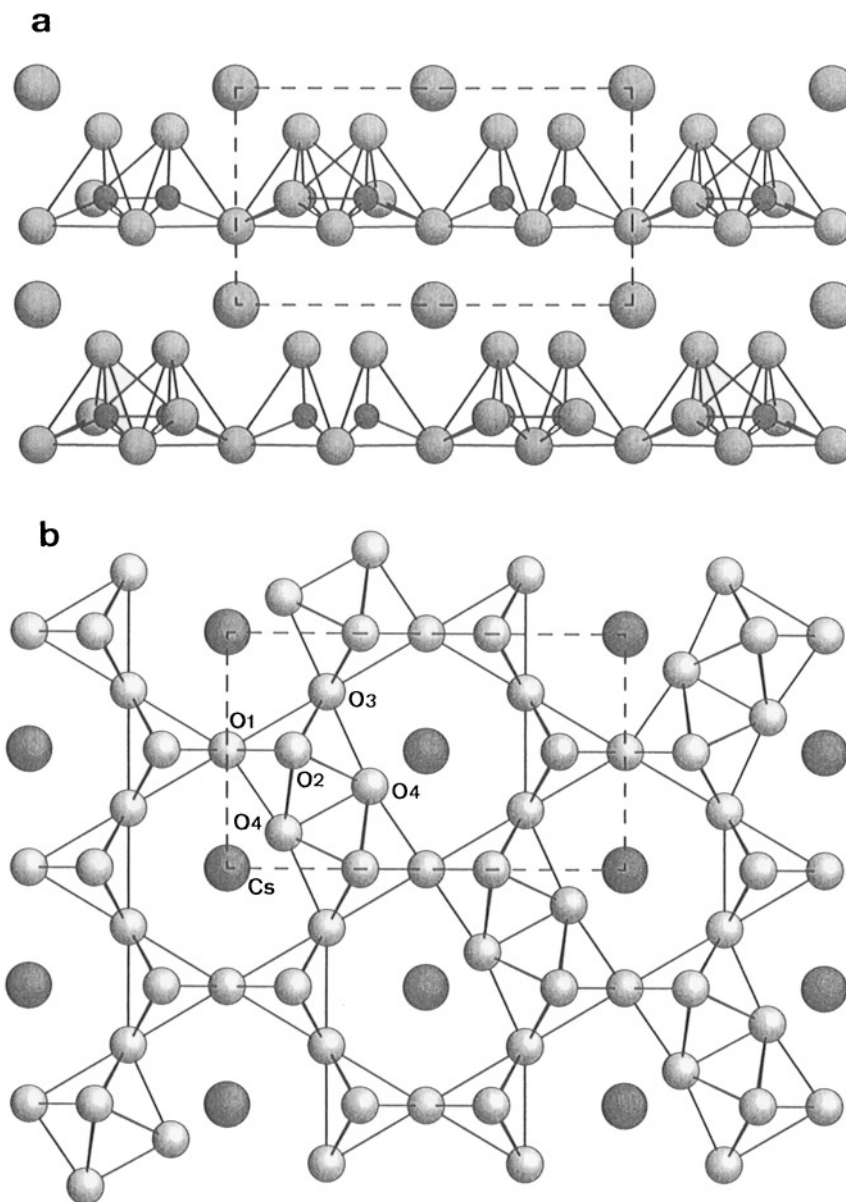
FIG. 3. Crystal structure of $Cs_2V_4O_{11}$ projected onto (a) the bc place and (b) the ab plane. Unit cell is denoted by broken lines.

Comparison with Structures of Other Cesium Vanadates

The structure of $Cs_2V_4O_{11}$ adds a new category of the V–O network structures of vanadate compounds. It is worthwhile to compare the present structure with those of other cesium vanadates, of which CsV_3O_8 (5, 8), $CsVO_3$ (4), and $CsVO_3 \cdot 0.5H_2O$ (10) with Cs/V ≤ 1 have V–O networks and $Cs_4V_2O_7 \cdot 2H_2O$ (11) with Cs/V = 2 has isolated $V_2O_7^{4-}$ ions. $CsVO_3$ and $CsVO_3 \cdot 0.5H_2O$ with Cs/V = 1 show similar V–O chains of vertex-sharing VO_4 tetrahedra: straight chains in $CsVO_3$ and zigzag chains in $CsVO_3 \cdot 0.5H_2O$. CsV_3O_8 with Cs/V = 1/3, on the other hand, has

a V_3O_8 layer with a rather complicated structure consisting of VO_6 octahedra and VO_5 trigonal bipyramids. The V_3O_8 layer is constructed in a manner that zigzag chains of edge-sharing VO_5–VO_5–VO_6 units are connected by sharing vertices. So the oxygen coordination numbers (CN) around V are CN = 4 for $CsVO_3$ and $CsVO_3 \cdot 0.5H_2O$ and CN = 5, 6 (average CN = 5.33) for CsV_3O_8. $Cs_2V_4O_{11}$ with Cs/V = 1/2, intermediate between 1 and 1/3, has a V_4O_{11} layer which is derived from the V_4O_{10} prototype layer (Fig. 1). The V_4O_{10} layer is made up of solely VO_4 tetrahedra (CN = 4) connecting through shared vertices and is structurally related to the tetrahedral silicate sheet of clay
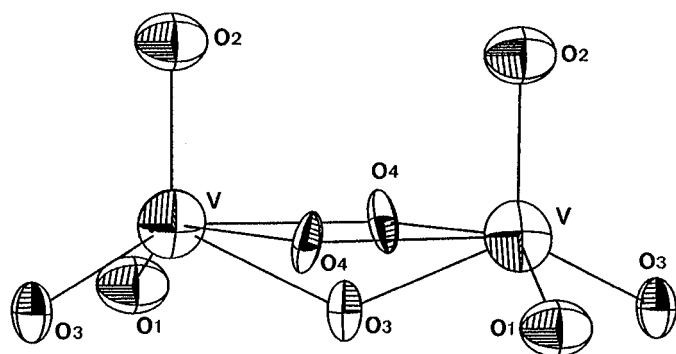
FIG. 4. V–O coordinations around adjacent V atoms showing vertex-sharing VO_4 tetrahedra and edge-sharing VO_5 trigonal bipyramids represented by thermal ellipsoids with 50% probability.

minerals (12); actually $Cs_2V_4O_{11}$ shows $b/a = 1.730$ being close to the ideal value of 1.732 for the tetrahedral silicate sheet. To add one oxygen to V_4O_{10}, one-fourth of the shared vertices are converted into the shared edges and thereby the CN changes from 4 to 5. Consequently $Cs_2V_4O_{11}$ consists of VO_4 tetrahedra and VO_5 trigonal bipyramids half-and-half to make CN = 4.5. In V–O frameworks of cesium vanadates, V–O polyhedra are VO_4 tetrahedron (CN = 4) for Cs/V = 1 and change partly to VO_5 trigonal bipyramids (CN = 5) for Cs/V = 1/2 and further to VO_6 octahedra (CN = 6) for Cs/V = 1/3. Isomorphous phases of $CsVO_3$ are found for Na, K, Rb, NH_4, and Tl to
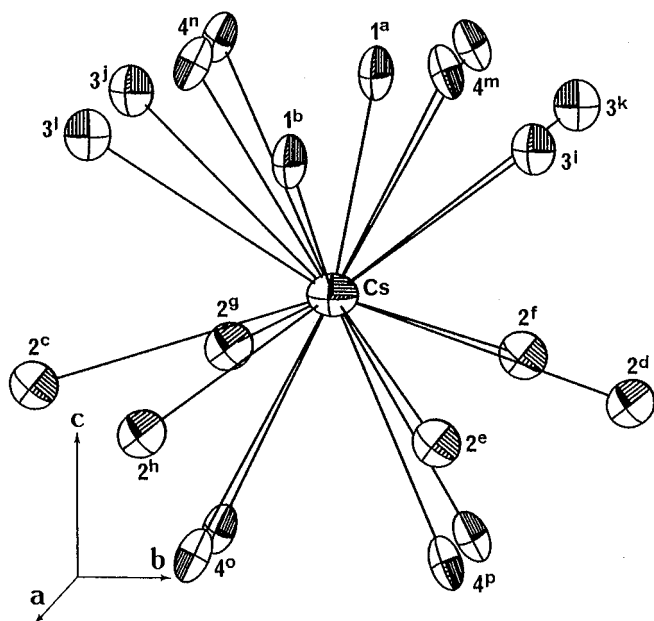

FIG. 5. Cs–O coordinations drawn with 50% thermal ellipsoids showing all the oxygens around Cs atom. Numbers and superscript letters for oxygens represent atom labels and symmetry codes, respectively, given in Table 5. Adjacent O(4) sites must not be occupied simultaneously.
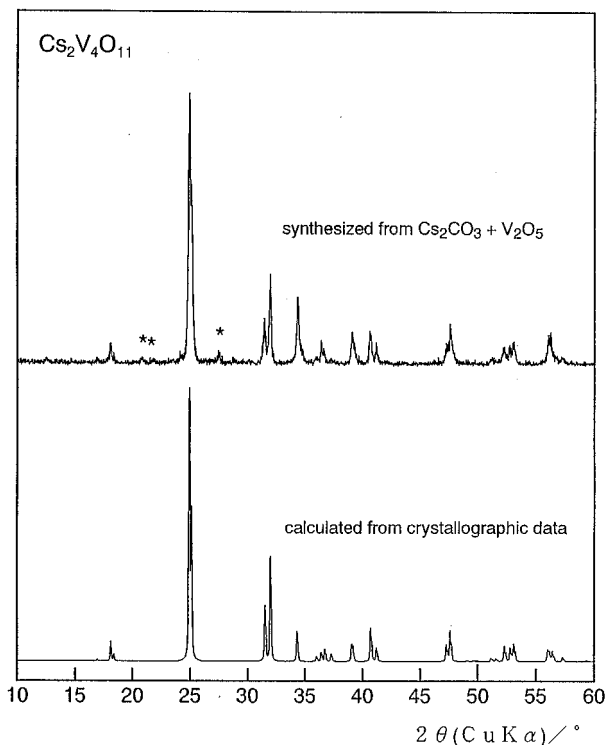

FIG. 6. Power X-ray diffraction patterns of $C_2V_4O_{11}$ synthesized from Cs_2CO_3 and V_2O_5 (top) and calculated from the present crystallographic data (bottom). Peaks marked with asterisks are assigned to impurity CsV_3O_8 phase.

replace Cs (4) and those of CsV_3O_8 for K, Rb, NH_4, and Tl (5–8). However, no isomorphous phase of $Cs_2V_4O_{11}$ has been known except for a possible candidate of $Rb_2V_4O_{11}$ (14) whose reported powder X-ray pattern with no indices can be indexed after the pattern of $Cs_2V_4O_{11}$ with the C-centered orthorombic system: $a = 5.66$ Å, $b = 9.56$ Å, and $c = 4.96$ Å. $Rb_2V_4O_{11}$ was assigned to a metastable phase obtained by solid state reaction of $RbNO_3$ and V_2O_5 (13) or by rapid cooling from completely fused samples (14) but has not been characterized yet. Further study to clarify the possible isomorphous candidate $Rb_2V_4O_{11}$ is now in progress.

ACKNOWLEDGMENT

REFERENCES

1. I. N. Belyaev and T. G. Golovanova, *Russ. J. Inorg. Chem.* **9,** 126 (1964).
2. J. Perraud, *Rev. Chim. Miner.* **11,** 302 (1974).
3. B. Forslund, *Chim. Scripta* **24,** 107 (1984).
4. F. C. Hawthrone and C. Calvo, *J. Solid State Chem.* **22,** 157 (1977).
5. H. T. Evans Jr. and S. Block, *Inorg. Chem.* **5,** 1808 (1966).

6. K-J. Range, C. Eglmeier, A. M. Heyns, and D. de Waal, Z. *Naturforsch. B* **45,** 31 (1990).

7. R. Benchrifa, M. Leblanc, and R. de Pape, *Acta Crystallogr. Sect. C* **46,** 177 (1990).

8. Y. Oka, T. Yao, and N. Yamamoto, *Mater. Res. Bull.* **32,** 1201 (1997).

9. "TEXSAN: Crystal Structure Analysis Package, Molecular Structure Corp." The Woodland, TX, 1985, 1992.

10. N. V. Avtamonova and V. K. Trunov, *J. Struct. Chem.* **32,** 147 (1991).

11. K. Kato and E. Takayama-Muromachi, *Acta Crystallogr. Sect. C* **41,** 163 (1985).

12. D. M. Moore and R. C. Reynolds Jr., "X-ray Diffraction and the Identification and Analysis of Clay Minerals." Oxford Univ. Press, New York, 1997.

13. L. Zúrková, V. Suchá, and K. Gápolovská, *J. Thermal Anal.* **20,** 17 (1981).

14. B. Forslund, *Chim. Scripta* **24,** 164 (1984).